Structural Engineering and Mechanics, Vol. 30, No. 2 (2008) 225-245
DOI: http://dx.doi.org/10.12989/sem.2008.30.2.225

A locally refinable T-spline finite element method for CAD/CAE integration

Tae-Kyoung Uhm

Department of Mechanical Engineering, KAIST, 373-1, Guseong-dong, Yuseong-gu, Daejeon 305-701, Korea

Ki-Seung Kim

Mechanical Engineering R&D Center, LIG Nex1, 148-1, Mabuk-dong, Giheung-gu, Yongin-si, Gyeonggi-do 449-910, Korea

Yu-Deok Seo and Sung-Kie Youn†

Department of Mechanical Engineering, KAIST, 373-1, Guseong-dong, Yuseong-gu, Daejeon 305-701, Korea

(Received September 17, 2007, Accepted July 23, 2008)

Abstract. T-splines are recently proposed mathematical tools for geometric modeling, which are generalizations of B-splines. Local refinement can be performed effectively using T-splines while it is not the case when B-splines or NURBS are used. Using T-splines, patches with unmatched boundaries can be combined easily without special techniques. In the present study, an analysis framework using T-splines is proposed. In this framework, T-splines are used both for description of geometries and for approximation of solution spaces. This analysis framework can be a basis of a CAD/CAE integrated approach. In this approach, CAD models are directly imported as the analysis models without additional finite element modeling. Some numerical examples are presented to illustrate the effectiveness of the current analysis framework.

Keywords: Non-Uniform Rational B-Splines (NURBS); T-splines; isogeometric analysis; finite element method; Computer-Aided Design (CAD); Computer-Aided Engineering (CAE).

1. Introduction

Finite element methods are versatile tools in the field of CAE. Although they have originated in 1950's, they have become nearly universal tools in industries and academies. They are essential tools for design of products such as automobiles, airplanes, vessels, etc. On the other hand, CAD has originated in 1970's. B-splines or NURBS are the primary mathematical tools to describe geometries in CAD while polynomials are mainly used in most finite element modeling. This

† Professor, Corresponding author, E-mail: skyoun@kaist.ac.krs

inconsistency makes the design process to be more complicated. In the conventional design process, CAD models are created first by designers according to function and productivity as well as aesthetics. These models are described by B-splines, NURBS, etc. and cannot be directly employed for engineering analysis owing to the inconsistency of mathematical expression of geometries. Therefore, engineers create analysis models separately. This modeling job entails discretization of geometries. This discretization is called meshing, a very cumbersome and time-consuming work. In the design process, the modification of CAD models frequently occurs and FE models should be reconstructed accordingly every time the CAD models are modified. The modification of FE models is also considerably expensive. In the design process of an automobile, a great deal of time and efforts are spent in the communication between CAD and CAE.

Another important point in the analysis is that the geometric exactness of CAD models is lost in the finite element modeling process. Curves or surfaces defined by splines in CAD models, are approximated by polynomials in FE models. This approximation of geometries can sometimes affect the accuracy of analysis.

These ineffectiveness and inaccuracy are originated from the different ways of geometric description in CAD and CAE. The reasonable solution to these problems is to unify languages of designers and engineers, namely their mathematical tools for geometric description. From the viewpoint of effective geometric modeling, the mathematical tools of CAD have more advantages. Geometric modeling is an intrinsic objective of CAD. Also, CAD industries are much larger than CAE. From these consideration, CAD based unification is more logical. By this unification, the process of product design can be innovated. Figs. 1 and 2 represent information flows in the conventional and CAD/CAE integrated product design, respectively. In the integrated approach, the finite element modeling is not necessary. CAD models can be directly used for engineering analysis. Reversely, the modification of geometries by means of design optimization could be reflected in CAD models at first hand. Communication between CAD and CAE is fairly easy since all geometries can be expressed using the same mathematical tools. In the engineering analysis, geometries are described exactly. Therefore, the errors of solutions which are generated from the

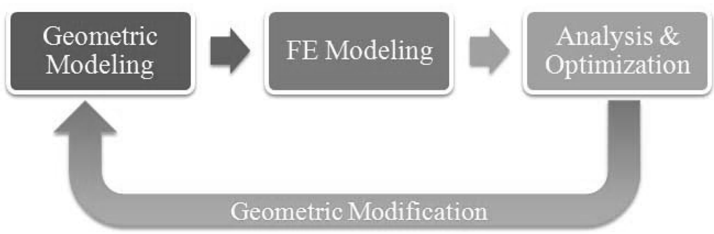

Fig. 1 Information flow in the conventional product design

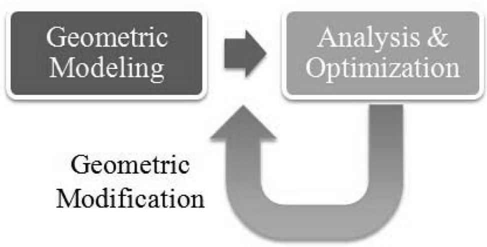

Fig. 2 Information flow in the CAD/CAE integrated product design

geometric approximation could be avoided.

Various approaches have been attempted to integrate CAD with CAE for certain structural analysis. Moore *et al.* (1984) introduced a quadrilateral shell element, in which the element geometry is described by rational B-spline functions in curvilinear coordinate system, while the displacement field is approximated by bi-cubic Hermite polynomials in Cartesian coordinates. Shen and Kan (1991) and Pengcheng and Peixiang (1995) developed multivariable spline element for the plate bending analysis. Fan and Luah (1993) have reported results of plate analysis as a special case of the B-spline finite element method restricted to cubic approximation. Cho and Roh (2003), and Roh and Cho (2004, 2005) proposed a framework that directly links shell finite element to B-spline surface geometric modeling. In their first works, NURBS surface data were used to calculate geometric properties such as curvature tensor. Later, NURBS were employed for even basis functions. This concept in which the solution space for dependent variables is represented in terms of the same functions which represent the geometry was named as the concept of isogeometric analysis by Hughes *et al.* (2005). Bazilevs *et al.* (2006), Cottrell *et al.* (2006, 2007) and Zhang *et al.* (2007) applied isogeometric analysis for various problems such as linear elasticity, fluid mechanics and dynamic problems. Natekar *et al.* (2004), Zhang and Subbarayan (2006), Zhang *et al.* (2007) and Rayasam *et al.* (2007) proposed partitioned, hierarchical analysis methodology called Constructive Solid Analysis (CSA). Inoue *et al.* (2005) performed shell analysis based on the NURBS representation. On the other hand, B-splines or NURBS are not necessary tools in isogeometric analysis. Cirak *et al.* (2000, 2001) and Cirak and Ortiz (2001) proposed the use of subdivision surfaces as a common foundation for modeling, simulation, and design in a unified framework.

Although B-splines or NURBS are the most widely used mathematical tools in computer graphics, they have certain limitations due to the use of parametric coordinates. When B-splines or NURBS are used, local refinement can be awkward and inefficient for both modeling and analysis. In the refinement process, many unnecessary control points are generated. For geometric modeling, those unwanted control points are quite annoying and for analysis, they induce unnecessary consumption of computational costs. Moreover, B-splines or NURBS are based on a rectangular parametric domain for the two-dimensional case. Because of this rectangle-shaped domain, B-spline or NURBS surfaces in the physical domain should have three- or four-sided geometries. Therefore, complex geometries consist of more than one patch. In this case, the interfaces between the patches should be seamless and have the same parametric spans. If not, many unnecessary control points should be generated to combine the patches. These limitations of finite element analysis using NURBS have to be solved in order to successfully apply it to industrial problems. In this paper, the use of T-splines is proposed both for description of geometries and for approximation of field variables. T-splines were proposed by Sederberg *et al.* (2003, 2004). A T-spline surface is a NURBS surface with T-junctions and is defined by a control grid called T-mesh. Details of T-splines will be reviewed later. The T-junctions enable T-spline surfaces to be refined locally. With this property, even patches with unmatched boundaries can be combined seamlessly.

This paper is organized as follows. In Section 2, we briefly introduce B-splines, NURBS and their properties. In Section 3, T-splines and their advantages will be reviewed. This is followed by description of an analysis framework based on NURBS and T-splines in Section 4. Some numerical examples and their results will be demonstrated in Section 5. Conclusions are summarized in Section 6.

2. B-splines and non-uniform rational B-splines (NURBS)

In this section, we briefly introduce B-splines, NURBS and their properties. Details can be found in (Piegl and Tiller 1997, Mortenson 2006, Rogers 2001). The properties of B-spline basis functions and rational basis functions presented here are very important because they are shape functions for finite element analysis as well as basis functions for geometric description.

2.1 B-spline basis functions

Let $S = \{s_0, \ldots, s_m\}$ be a nondecreasing sequence of real numbers, i.e., $s_i \le s_{i+1}$, $i = 0, \ldots, m-1$. The s_i are called knots, and S is the knot vector. The ith B-spline basis function of p-degree (order p+1) denoted by $N_{i,p}$, is defined as

$$N_{i,0}(s) = \begin{cases} 1 & \text{if} \quad s_i \le s < s_{i+1} \\ 0 & \text{otherwise} \end{cases} \tag{1a}$$

$$N_{i,p} = \frac{s - s_i}{s_{i+p} - s_i} N_{i,p-1}(s) + \frac{s_{i+p+1} - s}{s_{i+p+1} - s_{i+1}} N_{i+1,p-1}(s) \tag{1b}$$

Fig. 3 shows the generation of B-spline basis functions by this recursive formula. Here, important properties of the B-spline basis functions are presented. Assume degree p and a knot vector $S = \{s_0, \ldots, s_m\}$.

(1) Local support property; $N_{i,p}(s) = 0$ if s is outside the interval $[s_i, s_{i+p+1})$. This is illustrated by the Fig. 3.

(2) Partition of unity; for an arbitrary knot span, $[s_i, s_{i+1})$, $\sum_{j=i-p}^{i} N_{j,p}(s) = 1$ for all $s \in [s_i, s_{i+1})$.

(3) Smoothness; at a knot, $N_{i,p}(s)$ is $p-k$ times continuously differentiable, where k is the multiplicity of the knot.

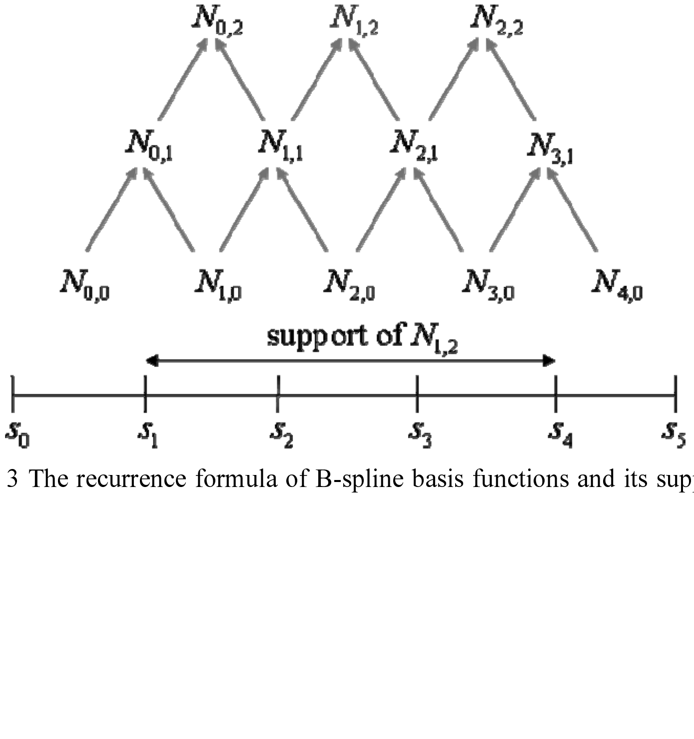

Fig. 3 The recurrence formula of B-spline basis functions and its support

2.2 B-spline curves

A pth-degree B-spline curve is defined by

$$\mathbf{C}(s) = \sum_{i=0}^{n} N_{i,p}(s)\mathbf{P}_i \quad 0 \le s \le 1 \tag{2}$$

where the $\{\mathbf{P}_i\}$ are control points, and the $\{N_{i,p}(s)\}$ the pth-degree B-spline basis functions defined on the nonperiodic knot vector $S = \{\underbrace{0, \dots, 0}_{p+1}, s_{p+1}, \dots, s_{m-p-1}, \underbrace{1, \dots, 1}_{p+1}\}$.

2.3 B-spline surfaces

A B-spline surface is obtained by taking a bidirectional net of control points, two knot vectors, and the products of the univariate B-spline functions

$$\mathbf{S}(s,t) = \sum_{i=0}^{n}\sum_{j=0}^{m} N_{i,p}(s)N_{j,q}(t)\mathbf{P}_{i,j} \tag{3}$$

with $S = \{\underbrace{0, \dots, 0}_{p+1}, s_{p+1}, \dots, s_{a-p-1}, \underbrace{1, \dots, 1}_{p+1}\}$, $T = \{\underbrace{0, \dots, 0}_{q+1}, t_{q+1}, \dots, t_{b-q-1}, \underbrace{1, \dots, 1}_{q+1}\}$. S and T have $a + 1$ and $b + 1$ knots, respectively.

2.4 NURBS curves and surfaces

Although polynomials offer many advantages, there exist a number of important curve and surface types which cannot be represented precisely using polynomials, e.g., circles, ellipses, hyperbolas, cylinders, cones, spheres, etc. They can be represented using rational functions, which are defined as the ratio of two polynomials. A rational curve in n-dimensional space can be represented by perspective mapping of a polynomial curve in (n+1)-dimensional space. By this mapping, a pth-degree NURBS curve can be represented as

$$\mathbf{C}(s) = \frac{\sum_{i=0}^{n} N_{i,p}(s)w_i\mathbf{P}_i}{\sum_{i=0}^{n} N_{i,p}(s)w_i} \quad 0 \le s \le 1 \tag{4}$$

where the $\{\mathbf{P}_i\}$ are the control points, the $\{w_i\}$ the weights, and the $\{N_{i,p}(s)\}$ the pth-degree B-spline basis functions defined on the nonperiodic (and nonuniform) knot vector $S = \{\underbrace{0, \dots, 0}_{p+1}, s_{p+1}, \dots, s_{m-p-1}, \underbrace{1, \dots, 1}_{p+1}\}$.

Setting

$$R_{i,p}(s) = \frac{N_{i,p}(s)w_i}{\sum_{j=0}^{n} N_{j,p}(s)w_j} \tag{5}$$

the Eq. (4) can be expressed in the form

$$\mathbf{C}(s) = \sum_{i=0}^{n} R_{i,p}(s)\mathbf{P}_i \tag{6}$$

The $\{R_{i,p}(s)\}$ are the rational basis functions. They are piecewise rational functions on $s \in [0, 1]$. The $R_{i,p}(s)$ have the following important properties.

(1) Partition of unity; $\sum_{i=0}^{n} R_{i,p}(s) = 1$ for all $s \in [0, 1]$
(2) Local support; $R_{i,p}(s) = 0$ for $s \notin [s_i, s_{i+p+1})$.
(3) Smoothness; All derivatives of $R_{i,p}(s)$ exist in the interior of a knot span. At a knot, $R_{i,p}(s)$ is $p-k$ times continuously differentiable, where k is the multiplicity of the knot.
(4) If $w_i = 1$ for all i, then $R_{i,p}(s) = N_{i,p}(s)$ for all i, i.e., the $N_{i,p}(s)$ are the special cases of the $R_{i,p}(s)$.

Rational basis functions for NURBS surfaces can be defined in an analogous way.

$$R_{i,j}(s,t) = \frac{N_{i,p}(s)N_{j,q}(t)w_{i,j}}{\sum_{k=0}^{n}\sum_{l=0}^{m} N_{k,p}(s)N_{l,q}(t)w_{k,l}} \tag{7}$$

And the NURBS surface can be written as

$$\mathbf{S}(s,t) = \sum_{i=0}^{n}\sum_{j=0}^{m} R_{i,j}(s,t)\mathbf{P}_{i,j} \tag{8}$$

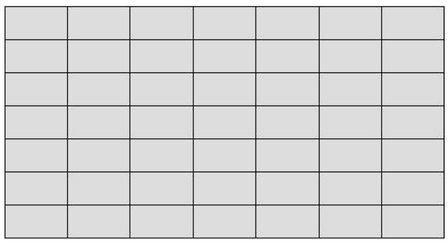

(a)

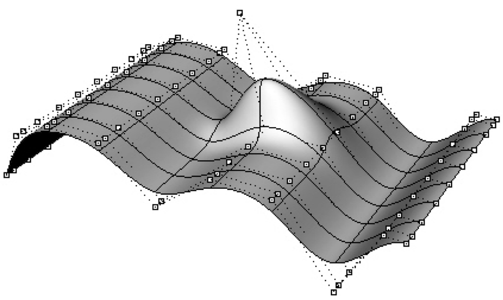

(b)

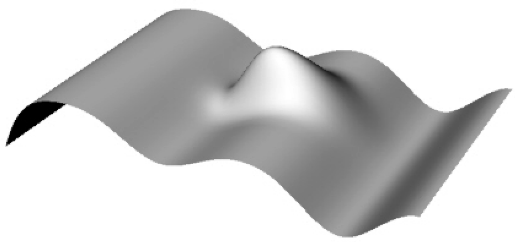

(c)

Fig. 4 An example of a bicubic NURBS surface: (a) parametric domain; (b) control net in physical domain; and (c) a NURBS surface

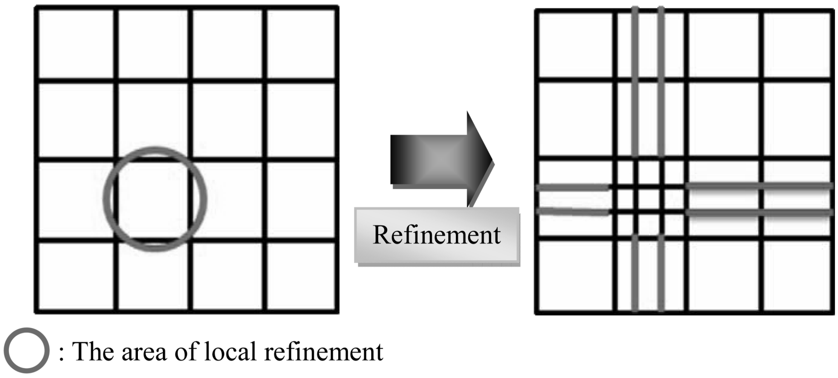

Fig. 5 Unwanted knot propagation of a NURBS surface for local refinement

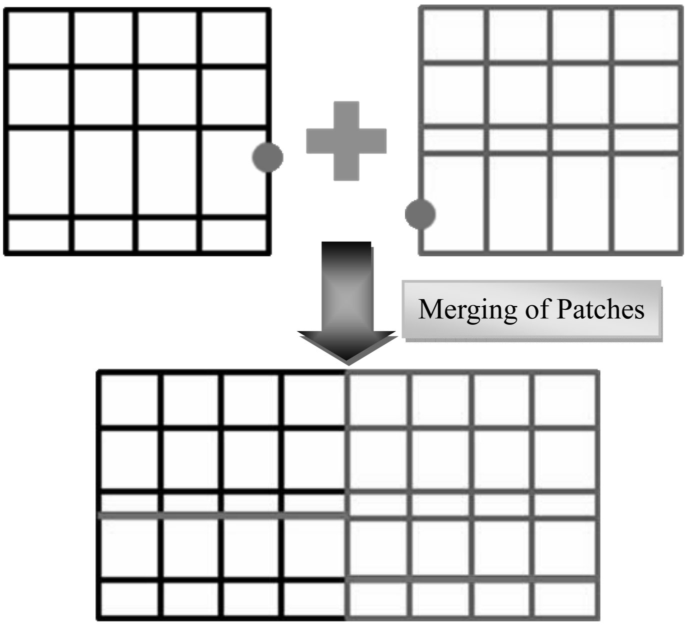

Fig. 6 Unwanted knot propagation of a NURBS surface for merging of patches

Fig. 4 shows an example of a bicubic NURBS surface. NURBS are the most widely used mathematical tools in computer graphics. Nonetheless, they have certain limitations. As stated before, local refinement is awkward and inefficient. Fig. 5 shows clearly this limitation of NURBS surfaces. When we try to refine a local area represented by a circle, knots are propagated from the local area to the boundaries of a domain. In this process, many superfluous control points are generated. It could be a burden for both modeling and analysis. Fig. 6 represents patch-merging process for NURBS surfaces. In this case, the two merging patches don't have the same knot spans in the merging boundary. During the merging process, knots are also propagated from one patch to the other, and unnecessary control points are created. These limitations of NURBS cast a shadow for the application of CAD/CAE integrated approach to industrial problems. In the following, we propose the use of T-splines instead of NURBS. Using T-splines, the limitations of NURBS can be removed completely.

3. T-splines

T-splines were proposed by Sederberg *et al.* (2003, 2004). They are some sort of PB (Point-Based)-splines. No topological relationship between control points exists for PB-splines. In this section, T-splines are briefly reviewed. The advantages of T-splines which NURBS doesn't have will be explained. Details of T-splines and their application for computer graphics can be found in (Sederberg *et al.* 2003, 2004, Song and Yang 2005, Guthe *et al.* 2005, Li *et al.* 2006).

3.1 T-spline surfaces

A T-spline is a NURBS surface with T-junctions and is defined by a control grid called T-mesh. The T-mesh is similar to a NURBS control grid except that T-junctions are allowed in the T-mesh. At T-junctions, a row or column of control points is terminated inside parametric domains. It is not possible for NURBS surfaces. Without T-junctions, T-spline surfaces are exactly the same as NURBS surfaces. Therefore, T-splines are generalizations of NURBS. The T-junctions enable T-spline surfaces to be refined locally. That is, it is possible to add a single control point to a T-spline control grid without propagating an entire row or column of control points and without altering the surface. The T-mesh is also associated with knot information of the T-spline, which is expressed using knot intervals indicating the difference between two knots and assigned to the edges of the T-mesh. The equation for a T-spline surface is

$$\mathbf{S}(s,t) = \frac{\sum_{i=0}^{n} B_i(s,t) w_i \mathbf{P}_i}{\sum_{i=0}^{n} B_i(s,t) w_i} \tag{9}$$

where the $\{\mathbf{P}_i\}$ are the control points, the $\{w_i\}$ the weights of control points. The T-spline basis function corresponding to control point $\mathbf{P}_i$ is $B_i(s,t)$ which is defined as follows:

$$B_i(s,t) = N_i^3(s) N_i^3(t) \tag{10}$$

where $N_i^3(s), N_i^3(t)$ are the cubic B-spline basis functions associated with the knot vectors $\mathbf{s}_i = [s_{i0}, s_{i1}, s_{i2}, s_{i3}, s_{i4}]$ and $\mathbf{t}_i = [t_{i0}, t_{i1}, t_{i2}, t_{i3}, t_{i4}]$, respectively. The knot vectors $\mathbf{s}_i$ and $\mathbf{t}_i$ are extracted from the T-mesh neighborhood of $\mathbf{P}_i$. NURBS is a special case of a T-spline. Therefore, the properties of rational basis functions of T-splines which are defined as

$$R_i(s,t) = \frac{B_i(s,t) w_i}{\sum_{j=0}^{n} B_j(s,t) w_j} \tag{11}$$

follow the properties of NURBS.

Refer to Fig. 7 for an example of a T-spline surface. Fig. 7(a) shows the T-mesh in the parametric domain where we can find two T-junctions. Fig. 7(b) shows its mapping image to the physical domain. Figs. 8-10 shows the advantages of T-splines. Firstly, Fig. 8 demonstrates flexibility of T-splines for local refinement. When we try to refine a local area represented by the circle, knots are propagated across the global domain in the case of NURBS. In this process, superfluous control

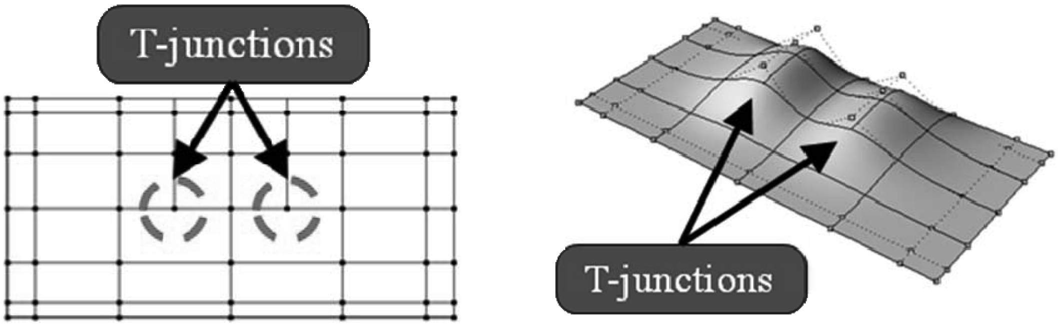

(a) T-mesh with two T-junctions (b) A T-spline surface in a physical domain

Fig. 7 An example of a T-spline surface

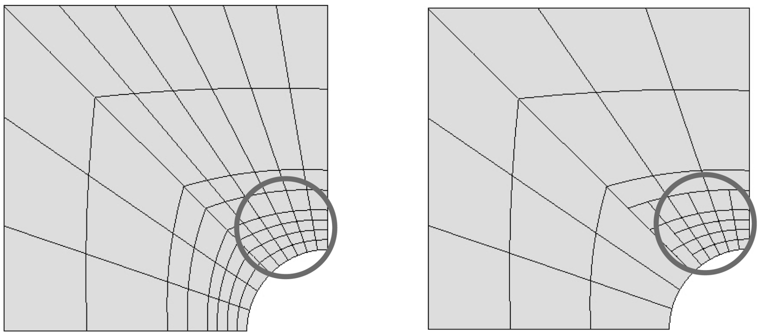

(a) A NURBS surface (234 control points) (b) A T-spline surface (174 control points)

Fig. 8 Comparison of T-spline and NURBS surfaces for local refinement

points are generated. The geometry is described by 234 control points in this case. Using T-splines, the area represented by the circle is only refined and propagation of knots are not caused. In this case, the geometry is described by only 174 control points. Although the difference in the number of control points here is not great, it could be tremendous for complex geometries. This effectiveness of T-splines for local refinement can greatly reduce inconvenience caused by superfluous control points in geometric modeling. Moreover, computational cost can be greatly decreased in analysis because control points represent DOFs. Fig. 9 represents patch-merging process using T-splines. This merging process for two NURBS surfaces yields one T-spline surface. As demonstrated in the figure, propagation of knots doesn't happen and no control points are generated. The unmatched knots in the merging boundary are treated by T-junctions. Fig. 10 also shows patch-merging process. In this case, geometries as well as knot spans of merging boundary are different for merging patches. As demonstrated in the figure, patches with unmatched knots and boundaries can be also easily combined. In this merging process, a compatibility problem doesn't exist. In industrial problems, complex structures with many sub-structures are sometimes designed by several people. In this procedure, there are many cases in which the interface of sub-structures is not matched. In conventional analysis, special techniques are needed to solve this problem. Using T-

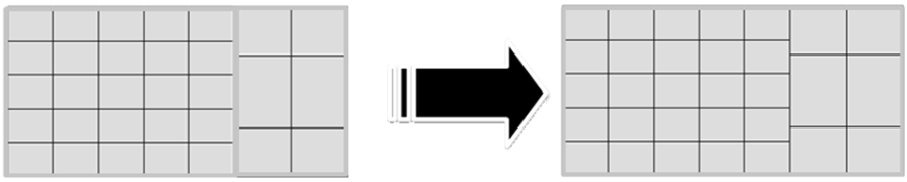

Fig. 9 Merging of two NURBS surfaces into one T-spline surface

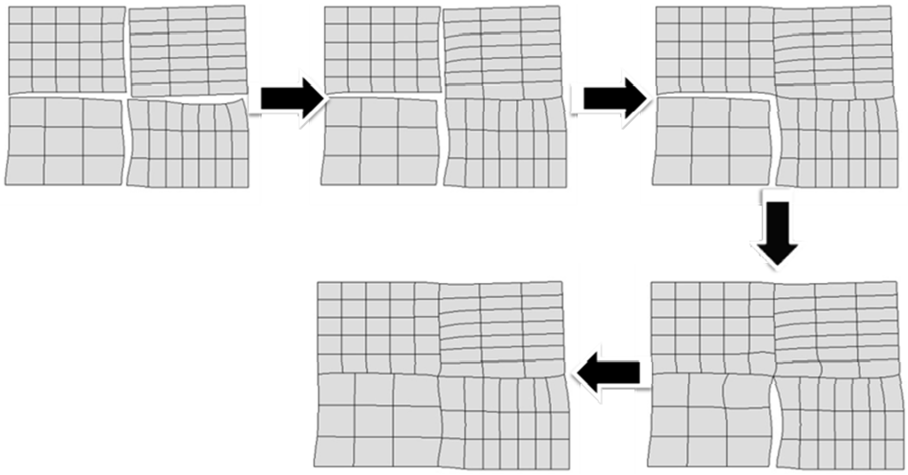

Fig. 10 A seamless patch merging process using T-splines

splines, analysis of complex structures with many sub-structures can be easily performed without special techniques.

The authors and their collaborators (Kim 2007, Kim *et al.* 2007, Uhm *et al.* 2007) applied T-splines to the finite element analysis for the first time. The developed T-spline finite element method is based on the CAD/CAE integrated approach and is the basis of this current study.

4. The analysis framework

The analysis framework used in the present study basically adopts the concept of isogeometric analysis by Hughes *et al.* (2005). It will be reviewed in this section. The analysis framework based on NURBS or T-splines for CAD/CAE integration consists of the followings.

(1) Expression of the geometry: The control points associated with the basis functions define the geometry. The geometry is represented in the parametric form. There exist the parametric domain and the corresponding physical domain. Fig. 11 represents the relation between the domains.

(2) Approximation of field variables: The fields are represented by the same basis functions as the geometry. Every control point has each basis function. The coefficients of the basis functions are the degrees-of-freedom, or control variables.

(3) Meshes and elements: A mesh is defined by the product of knot vectors, and elements are defined by knot spans. The shaded area as shown in Fig. 11 represents an element in the parametric and physical domains.

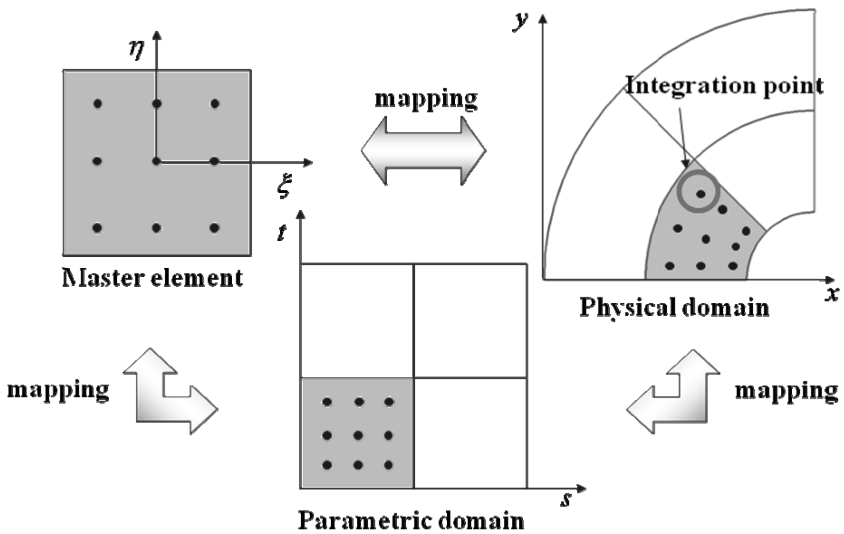

Fig. 11 Mapping relation between domains

(4) Support of basis functions: The support of basis functions is determined by the degree of basis functions and knot vectors. For example, a B-spline basis function $N_{i,p}(s)$ of p-degree has non-zero value only if s is within the interval $[s_i, s_{i+p+1})$.

(5) Mesh refinement: Global and local refinement can be done. Using NURBS, classical h-refinement can be performed by knot insertion. Elevating the degree of NURBS or T-splines, p-refinement also can be done. Using T-splines, control points can be inserted locally.

(6) Imposition of B.C.s: The Kronecker delta property is not satisfied by NURBS and T-splines. Nonetheless, imposition of essential B.C. is not a big problem. In our approach, we consider only nonperiodic (or clamped or open) knot vectors, in which their first and last knots appear $p+1$ times. Using nonperiodic knots, the Kronecker delta property is satisfied at the boundary and essential B.C.s can be imposed easily. Natural B.C.s can be imposed in the same way as in the standard finite element method.

(7) Integration: The integration is performed by the classical Gaussian quadrature within a master element. Fig. 11 shows the mapping relation among the master element, the element in the parametric domain and the element in the physical domain. Hughes *et al.* (2005) referred to the rule of thumb to use the lowest-order rule that would exactly integrate the integrand assuming the NURBS are B-splines of the same polynomial order and the Jacobian determinants are constants. In the present study, we propose to use higher-order rule instead of the lowest-order rule because NURBS or T-splines are the rational functions and cannot be exactly integrated with the same-order rule as for polynomials. More research needs to be done for robust quadrature rule.

The NURBS or T-spline finite element method follows the basic line of a classical finite element method. To clarify the differences and similarities between the two methods, they are compared in Table 1.

The general procedure for spline-based finite element methods is shown in Fig. 12. Firstly, geometric information is taken from CAD data and information for analysis is given. Then, global

Table 1 The comparison of the conventional and spline-based FEM

Conventional FEM	Spline-based FEM
Nodal points	Control points
Mesh	Knots
Polynomial	NURBS or T-splines
Approximate geometry	Exact geometry
Partition of unity (O)	Partition of unity (O)
Compact support (O)	Compact support (O)
Kronecker delta prop. (O)	Kronecker delta prop. (X)

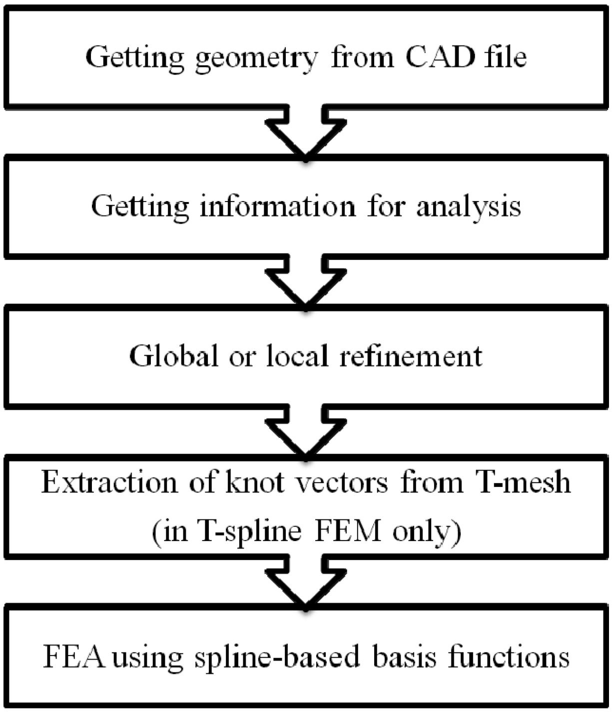

Fig. 12 General procedure of the spline-based finite element method

or local refinement is performed. Refinement is generally necessary because enough control points for analysis is not obtained with only CAD models. In our study, global refinement of NURBS surfaces by knot insertion is preceded. Then, the conversion of NURBS surfaces into T-spline surfaces is performed. Local refinement of T-spline surfaces by addition of control points follows. After refinement, the extraction of knot vectors for every control points is done for the case of the T-spline finite element method. Finally, the finite element analysis is performed using spline-based basis functions.

For NURBS and T-spline finite element methods, there are gains and losses in terms of computational efficiency. In these methods, the shape functions of control points must be computed for each control point while it doesn't change in the conventional finite element method. The shape functions have the rational polynomial form in these methods, and higher quadrature rule may be used for exact integration. For T-splines, there is one more step in the analysis procedure, that is, the extraction of knot vectors from T-mesh. These factors demand more computational efforts than the conventional finite element method does. There are also gains in the computational efficiency. Generally, less DOFs are required for the same level of accuracy by using NURBS or T-spline finite element method. It means that the time for solving linear equations can be reduced with relation to the conventional finite element method. For the quadratic case, meshes in the NURBS and conventional finite element methods are compared in Fig. 13, where each mesh is composed of the same number of elements. For the NURBS finite element method, DOFs are approximately proportional to $(n+2)^2$ while they are approximately proportional to $(2n+1)^2-n^2$ for the conventional finite element method, where n is the number of elements. Therefore, the smaller number of DOFs are required to construct the mesh with the same number of elements in the case of NURBS finite element method. The problem of the infinite plate with a circular hole of Fig. 14 is solved by the NURBS and conventional finite element method, and the computational time and accuracy are compared in Table 2. For the same number of elements, approximately three times more DOFs are required in the conventional finite element method. To construct the stiffness matrix, roughly three times more time is required for the NURBS finite element method. This is

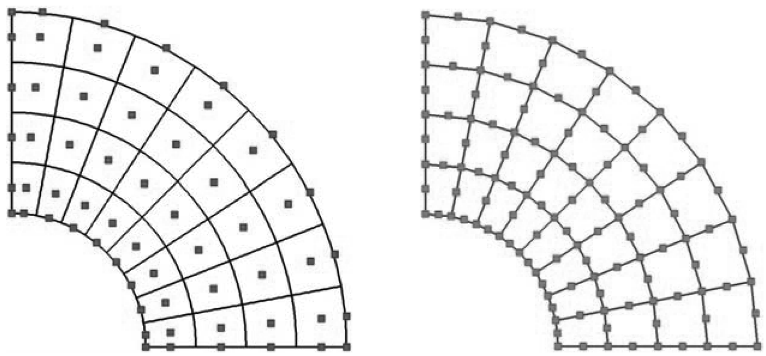

(a) (b)

Fig. 13 The comparison of the (a) NURBS and (b) conventional finite element meshes for the quadratic case

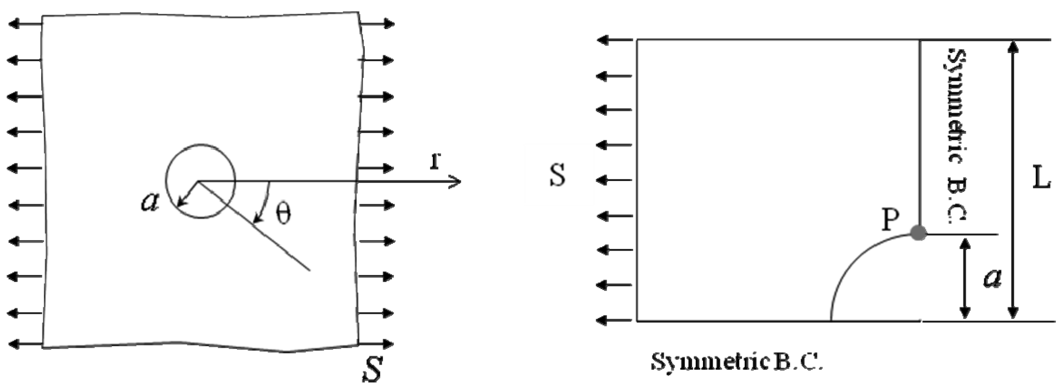

(a) (b)

Fig. 14 (a) Infinite plate with a circular hole under a uniform tension and (b) its 1/4 model

Table 2 The comparison of computational efficiency for the NURBS and conventional FEM

	Conventional FEM	NURBS FEM
The number of DOFs	49922	17292
Time for constructing the stiffness matrix	0.1281 (s)	0.3422 (s)
Time for solving the linear equation	1.8563 (s)	0.9218 (s)
The relative L^2-norm of stresses	4.010E-4	4.109E-4

attributed to the factors as stated before. For the time to solve the linear equation, only half time is enough for the NURBS finite element method because the number of DOFs is much less. In this problem, the domain-wise multi-frontal solver (Kim *et al.* 2005) is employed for solving the linear equation. The L^2-norm of stresses for the two methods is comparable. The only difference in the analysis procedure between the NURBS and T-spline finite element methods is the extraction of knot vectors from the T-mesh. This is not a costly job, and the overall properties of the T-spline finite element method in terms of computational efficiency are similar with the NURBS case.

5. Numerical examples

Consider a 2-D linear elasticity problem in the domain Ω bounded by Γ. The equilibrium equations are

$$\sigma_{ij,j} + b_i = 0 \quad \text{in} \quad \Omega \tag{12}$$

where $\sigma_{ij,j}$ is the Cauchy stress tensor and b_i is the body force. The boundary conditions are as follows:

$$\sigma_{ij} n_j = \bar{t}_i \quad \text{on } \Gamma_t \tag{13}$$

$$u_i = \bar{u}_i \quad \text{on } \Gamma_u \tag{14}$$

where $\bar{t}_i$ is the prescribed traction on a surface, and $\bar{u}_i$ the prescribed displacement field, n_j the unit outward normal to the boundary Γ. Γ_t and Γ_u are complementary subsets of Γ.

5.1 Infinite plate with a circular hole under a uniform tension

In this two-dimensional example, the effectiveness of local refinement using T-splines is demonstrated. Fig. 14(a) describes this problem in which the infinite plate with a circular hole is loaded under a uniform tension. The exact solution of this problem can be found in the Reference [Timoshenko and Goodier 1987, pp.90-92].

$$\sigma_r(r, \theta) = \frac{S}{2}\left(1 - \frac{a^2}{r^2}\right) + \frac{S}{2}\left(1 - \frac{4a^2}{r^2} + \frac{3a^4}{r^4}\right)\cos 2\theta \tag{15}$$

$$\sigma_\theta(r, \theta) = \frac{S}{2}\left(1 + \frac{a^2}{r^2}\right) - \frac{S}{2}\left(1 + \frac{3a^4}{r^4}\right)\cos 2\theta \tag{16}$$

$$\tau_{r\theta}(r,\theta) = -\frac{S}{2}\left(1+\frac{2a^2}{r^2}-\frac{3a^4}{r^4}\right)\sin 2\theta \tag{17}$$

where S is the magnitude of the applied tensile stress. Because of the symmetry, only 1/4 model is considered as shown in the Fig. 14(b). L is the length of the finite quarter plate, a the radius of the hole. In this problem, we use $L = 4$, $a = 1$, and $S = 10$. For material properties, $E = 10^5$ and $\nu = 0.3$ are used. At the point P in the Fig. 14(b), stress concentration is anticipated. From the exact solution, $\sigma_x = 30$ is expected at this point (at $r = a$, $\theta = 3\pi/2$) of the infinite plate.

This problem is solved by NURBS and T-spline finite element methods. Fig. 15 shows the respective mesh configurations. Using T-splines, local refinement is performed around the point of stress concentration. This local refinement is not implemented adaptively, but done empirically. The systematic adaptive local refinement is our future work. Using NURBS, h-refinement by knot insertion is done. It is refined globally. The first mesh configurations of T-splines and NURBS are the same. As stated before, a T-spline is a generalization of NURBS. With no T-junctions, T-spline surfaces are exactly NURBS surfaces. In all the problems in this study, cubic NURBS and T-splines are used. Fig. 16 shows the contour plot of σ_x and deformed shape obtained from the analysis. Stress concentration is observed at the point P. Detailed numerical results are summarized in Table 3 and the convergence of two methods is compared in Fig. 17. As demonstrated in Fig. 17 and Table 3, the spline-based finite element methods converge faster than the conventional finite element method. Comparing the results for T-splines and NURBS, the T-spline finite element method converges faster than the NURBS finite element method. This result shows the great effectiveness of T-splines. Using T-splines, only necessary control points can be locally added in the

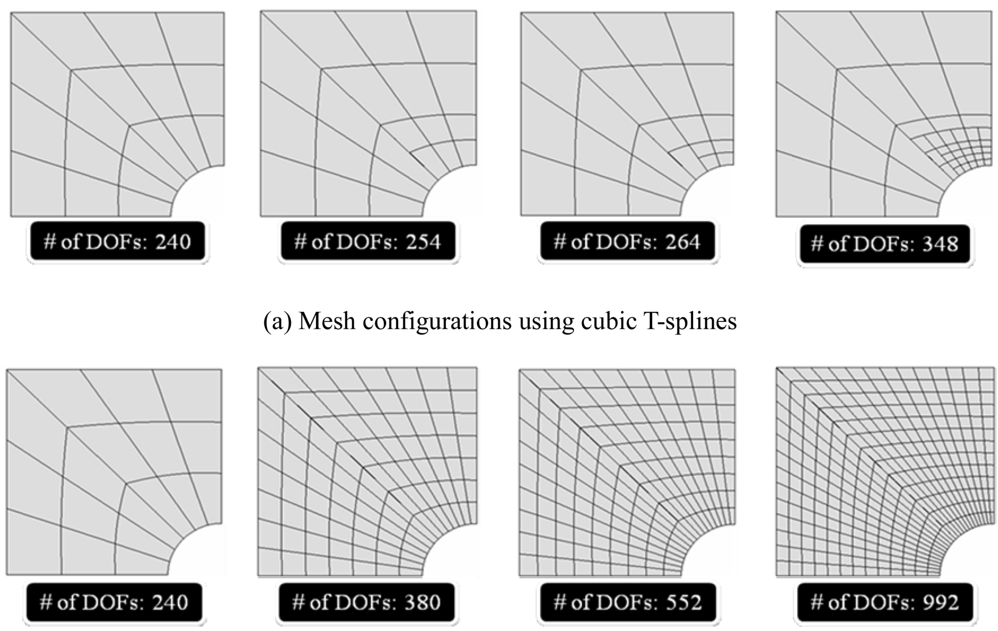

(a) Mesh configurations using cubic T-splines

(b) Mesh configurations using cubic NURBS

Fig. 15 (a) Meshes produced by local refinement of T-splines and (b) Meshes produced by h-refinement of NURBS

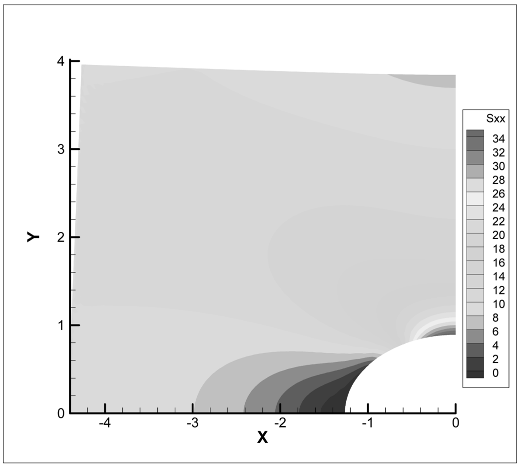

Fig. 16 The contour plot of σ_x and the deformed shape obtained from the analysis

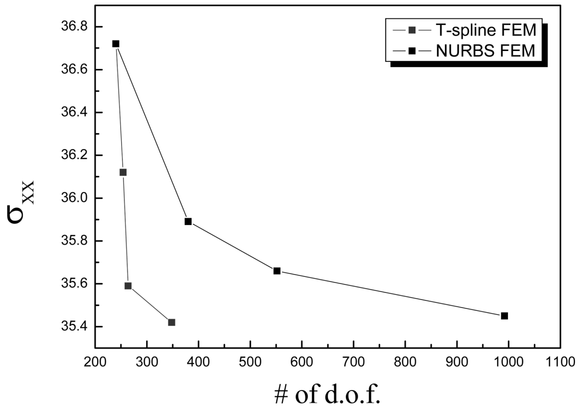

Fig. 17 The comparison of convergence for the T-spline and NURBS finite element methods

Table 3 Numerical results from the spline-based and conventional FEM

Case	# of DOFs	σ_x
T-spline FEM 1	240	36.72
T-spline FEM 2	254	36.12
T-spline FEM 3	264	35.59
T-spline FEM 4	348	35.42
NURBS FEM 1	240	36.72
NURBS FEM 2	380	35.89
NURBS FEM 3	552	35.66
NURBS FEM 4	992	35.45
Conventional FEM 1	266	36.16
Conventional FEM 2	1290	36.05
Conventional FEM 3	2562	35.96
Conventional FEM 4	5642	35.90

right place. With NURBS, unnecessary control points are added together with the necessary ones.

5.2 Bending of a curved bar by a force at the end

The problem setup is presented in Fig. 18. A curved bar is under bending by a force at the end. The other end is fixed. In this problem, a = 2, b = 3 and P = 10 are used. For material properties, E = 10^5 and ν = 0.3 are used.

Fig. 19 shows the mesh configuration used for analysis. It is generated from local refinement of a NURBS surface. Fig. 20 shows the analysis results, the contours of Von-Mises stresses and the deformed shapes of the curved bar. The maximum Von-Mises stress from the T-spline finite element method is 194.3. This result is very similar to the one from conventional finite element method. The maximum Von-Mises stress from the conventional finite element method is 193, and quadratic

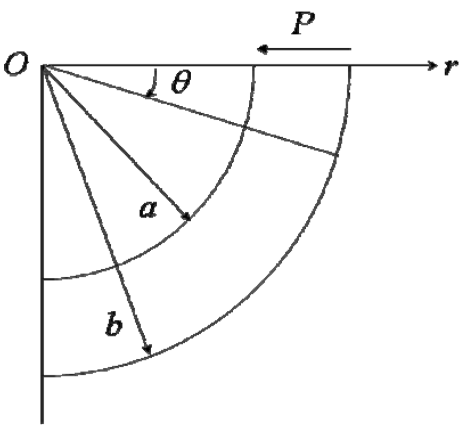

Fig. 18 The bending of a curved bar by a force at the end

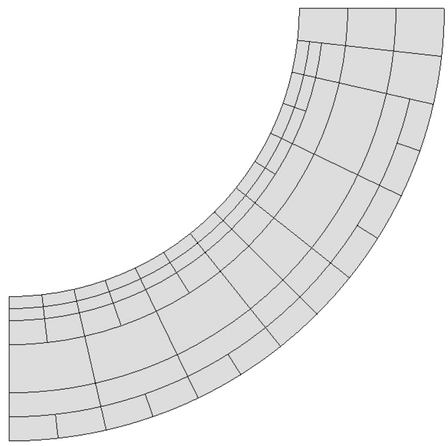

Fig. 19 The mesh configuration produced by local refinement

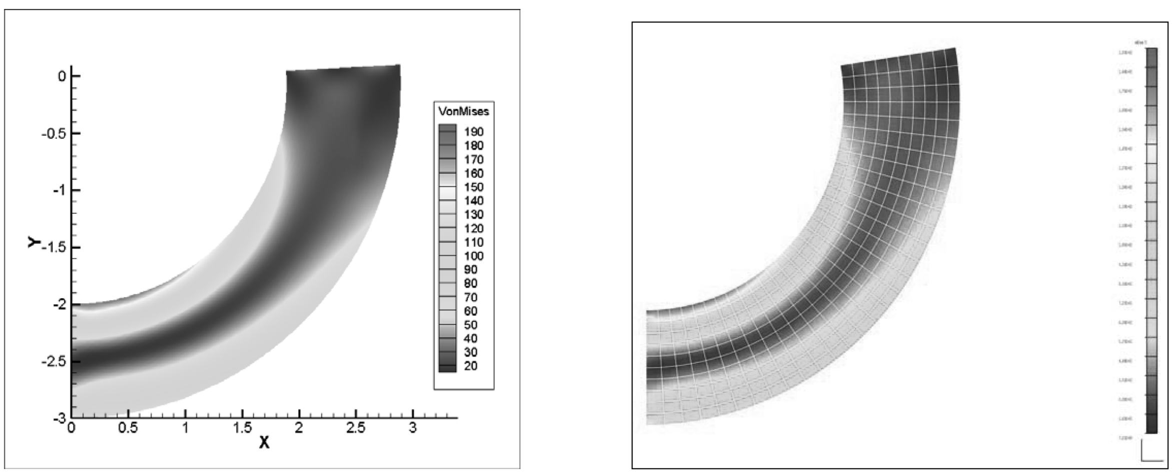

(a) (b)

Fig. 20 The contour plots of Von-Mises stresses and the deformed shapes of the curved bar from the (a) T-spline and (b) conventional FEM

elements are used for comparison.

5.3 Clevis under a uniform tension

This problem shows the effectiveness of patch-merging process using T-splines. The problem specification is shown in Fig. 21. A clevis is under a uniform tension (P = 10). Because of symmetry, only 1/2 model is considered. The homogeneous essential B.C. is imposed in the inner hole of the clevis. For material properties, $E = 10^5$ and $\nu = 0.3$ are used. In this problem, the half model of the clevis have six sides. To make this with one NURBS patch is inconvenient. This is modeled with two NURBS patches as shown in Fig. 22(a). The knot spans in the merging boundary is not matched in this case. For analysis, the two patches should be merged, or some special

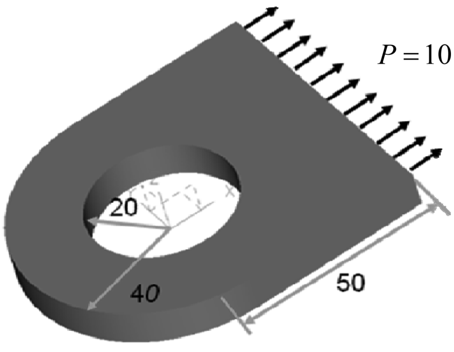

Fig. 21 The clevis under a uniform tension

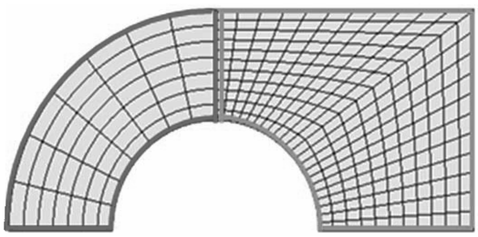

(a) Two NURBS patches

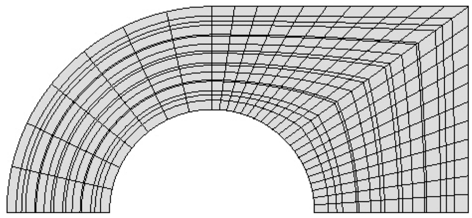

(b) Merging into one NURBS patch (740 control points)

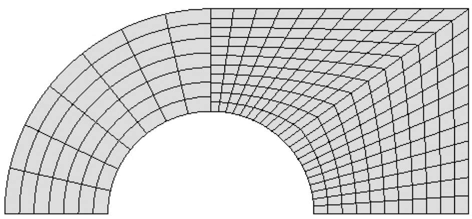

(c) Merging into one T-spline patch (474 control points)

Fig. 22 The comparison of patch-merging process for NURBS and T-splines

techniques are needed. Using NURBS, the two unmatched patches are merged as shown in the Fig. 22(b). In this merging process, propagation of knots from one patch to the other is caused. Consequently, the model is described by 740 control points. Using T-splines, the model can be represented by only 474 control points as demonstrated in the Fig. 22(c). In this problem, the analysis is performed using T-splines and the result is shown in Fig. 23(a). It shows the contour of Von-Mises stresses and the deformed shape of the clevis. No jump of stresses and no incompatible modes are observed in the merging boundary. Once again, this result is compared with the one from the conventional finite element method as shown in Fig. 23(b). The maximum Von-Mises stress is 15.91 for the T-spline finite element method and 15.90 for the conventional finite element method. They show almost identical results. Merging of subdomains or patches is often required for the real problems of industries. The T-splines finite element method again shows its great ability in these kinds of problems.

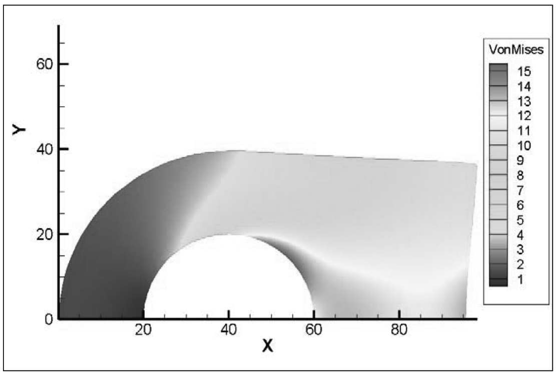

(a)

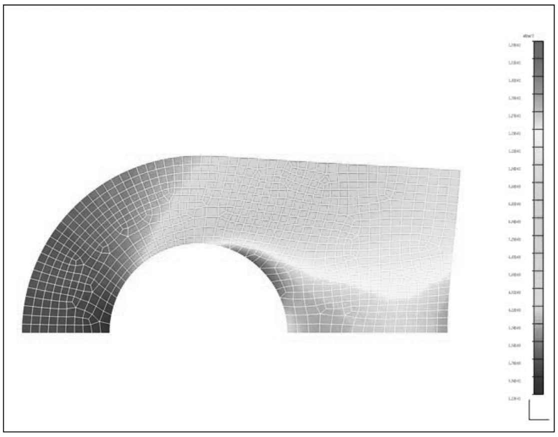

(b)

Fig. 23 The contour plots of Von-Mises stresses and the deformed shapes of the clevis from the (a) T-spline and (b) conventional FEM

6. Conclusions

In the present study, an analysis framework using T-splines was proposed. In this framework, T-splines are used to describe geometries and approximate field variables. The key feature of T-splines is the ability of local refinement. Moreover, patch merging can be flexibly implemented. These flexibility and effectiveness of T-splines were applied to finite element analysis. In this analysis, CAD models were directly used without additional finite element modeling. Some numerical examples were presented. More research needs to be done to apply this analysis framework to industrial problems. A scheme of adaptive local refinement should be developed. Various analysis problems including three-dimensional or shell problems need to be solved. Complex structures comprised of many sub-structures need to be treated effectively. In conclusion, this analysis framework using T-splines has considerable potential in practical problems and is a very promising alternative to conventional analysis framework.

Acknowledgements

This work was supported by the Korea Research Foundation Grant funded by the Korean Government (MOEHRD, Basic Research Promotion Fund) (KRF-2007-313-D00024).

References

Bazilevs, Y., Calo, V.M., Zhang, Y. and Hughes, T.J.R. (2006), "Isogeometric fluid-structure interaction analysis with applications to arterial blood flow", *Comput. Mech.*, **38**, 310-322.

Cho, M. and Roh, H.Y. (2003), "Development of geometrically exact new shell elements based on general curvilinear co-ordinates", *Int. J. Numer. Meth. Eng.*, **56**, 81-115.

Cirak, F. and Ortiz, M. (2001), "Fully C^1-conforming subdivision elements for finite deformation thin-shell analysis", *Int. J. Numer. Meth. Eng.*, **51**, 813-833.

Cirak, F., Ortiz, M. and Schrder, P. (2000), "Subdivision surfaces: a new paradigm for thin-shell finite-element analysis", *Int. J. Numer. Meth. Eng.*, **47**, 2039-2072.

Cirak, F., Scott, M.J., Antonsson, E.K., Ortiz, M. and Schrder, P. (2002), "Integrated modeling, finite-element analysis, and engineering design for thin-shell structures using subdivision", *Comput. Aided Des.*, **34**, 137-148.

Cottrell, J.A., Hughes, T.J.R. and Reali, A. (2007), "Studies of refinement and continuity in isogeometric structural analysis", *Comput. Meth. Appl. Mech. Eng.*, **196**, 4160-4183.

Cottrell, J.A., Reali, A., Bazilevs, Y. and Hughes, T.J.R. (2006), "Isogeometric analysis of structural vibrations", *Comput. Meth. Appl. Mech. Eng.*, **195**, 5257-5296.

Fan, S.C. and Luah, M.H. (1993), "Nine node spline element for free vibration analysis of general plates", *J. Sound Vib.*, **165**, 85-100.

Guthe, M., Balazs, A. and Klein, R. (2005), "GPU-based trimming and tessellation of NURBS and T-Spline surfaces", *ACM T. Graphic.*, **24**, 1016-1023.

Hughes, T.J.R., Cottrell, J.A. and Bazilevs, Y. (2005), "Isogeometric analysis: CAD, finite elements, NURBS, exact geometry and mesh refinement", *Comput. Meth. Appl. Mech. Eng.*, **194**, 4135-4195.

Inoue, K., Kikuchi, Y. and Masuyama, T. (2005), "A NURBS finite element method for product shape design", *J. Eng. Des.*, **16**, 157-174.

Kim, J.H., Lee, C.S. and Kim, S.J. (2005), "High-performance domain-wise parallel direct solver for large-scale structural analysis", *AIAA J.*, **43**, 662-670.

Kim, K.-S. (2007), *A study on T-spline Finite Element Analysis with Local Refinement*, M.S. Dissertation, KAIST.

Kim, K.-S., Seo, Y.-D. and Youn, S.-K. (2007), "Spline-based finite element analysis with T-spline local refinement", *Proceeding of the International Conference on Computational Methods (ICCM 2007)*, Hiroshima, Japan, p. 188.

Li, C.J., Wang, R.H. and Zhang, F. (2006), "Improvement on the dimensions of spline spaces on T-Mesh", *J. Inf. Comput. Sci.*, **3**, 235-244.

Moore, C.J., Yang, T.Y. and Anderson, D.C. (1984), "New 48 D.O.F. quadrilateral shell element with variable-order polynomial and rational B-spline geometries with rigid body modes", *Int. J. Numer. Meth. Eng.*, **20**, 2121-2141.

Mortenson, M.E. (2006), *Geometric Modeling*, Industrial Press Inc., New York, NY.

Natekar, D., Zhang, X. and Subbarayan, G. (2004), "Constructive solid analysis: A hierarchical, geometry-based meshless analysis procedure for integrated design and analysis", *Comput. Aided Des.*, **36**, 473-486.

Pengcheng, S. and Peixiang, H. (1995), "Bending analysis of plates and spherical shells by multivariable spline element method based on generalized variational principle", *Comput. Struct.*, **55**, 151-157.

Piegl, L.A. and Tiller, W. (1997), *The NURBS Book (monographs in visual communication)*, Springer-Verlag , New York, NY.

Rayasam, M., Srinivasan, V. and Subbarayan, G. (2007), "CAD inspired hierarchical partition of unity constructions for NURBS-based, meshless design, analysis and optimization", *Int. J. Numer. Meth. Eng.*, **72**, 1452-1489.

Rogers, D.F. (2001), *An Introduction to NURBS with Historical Perspective*, Academic Press, San Diego, CA.

Roh, H.Y. and Cho, M. (2004), "The application of geometrically exact shell elements to B-spline surfaces", *Comput. Meth. Appl. Mech. Eng.*, **193**, 2261-2299.

Roh, H.Y. and Cho, M. (2005), "Integration of geometric design and mechanical analysis using B-spline functions on surface", *Int. J. Numer. Meth. Eng.*, **62**, 1927-1949.

Sederberg, T.W., Cardon, D.L., Finnigan, G.T., North, N.S., Zheng, J. and Lyche, T. (2004), "T-spline simplification and local refinement", *ACM T. Graphic.*, **23**, 276-283.

Sederberg, T.W., Zheng, J., Bakenov, A. and Nasri, A. (2003), "T-splines and T-NURCCs", *ACM T. Graphic.*, **22**, 477-484.

Shen, P.-C. and Kan, H.-B. (1991), "Multivariate spline element analysis for plate bending problems", *Comput. Struct.*, **40**, 1343-1349.

Song, W. and Yang, X. (2005), "Free-form deformation with weighted T-spline", *Visual Comput*., **21**, 139-151.

Timoshenko, S.P. and Goodier, J.N. (1987), *Theory of Elasticity*, McGraw-Hill, New York, NY.

Uhm, T.-K., Seo, Y.-D., Kim, H.-J. and Youn, S.-K. (2007), "T-spline finite element method with local refinement", *Proceedings of 9th U.S. National Congress on Computational Mechanics*, San Francisco, U.S., p. 291.

Zhang, X. and Subbarayan, G. (2006), "jNURBS: An object-oriented, symbolic framework for integrated, meshless analysis and optimal design", *Adv. Eng. Softw.*, **37**, 287-311.

Zhang, X., Rayasam, M. and Subbarayan, G. (2007), "A meshless, compositional approach to shape optimal design", *Comput. Meth. Appl. Mech. Eng.*, **196**, 2130-2146.

Zhang, Y., Bazilevs, Y., Goswami, S., Bajaj, C.L. and Hughes, T.J.R. (2007), "Patient-specific vascular NURBS modeling for isogeometric analysis of blood flow", *Comput. Meth. Appl. Mech. Eng.*, **196**, 2943-2959.